Available online at www.sciencedirect.com
ScienceDirect
Organic Geochemistry 37 (2006) 1278–1288
Organic Geochemistry
www.elsevier.com/locate/orggeochem

Insights from stable S and O isotopes into biogeochemical processes and genesis of Lower Cambrian barite–pyrite concretions of South China

Tatiana Goldberg [a,c,*], Aninda Mazumdar [b], Harald Strauss [a], Graham Shields [c]

[a] *Geologisch-Paläontologisches Institut, Westfälische Wilhelms Universität, Corrensstrasse 24, 48149 Münster, Germany*
[b] *National Institute of Oceanography (NIO), Dona Paula, Goa, India*
[c] *School of Earth Sciences, James Cook University, Townsville, Qld. 4811, Australia*

Received 2 August 2005; received in revised form 26 January 2006; accepted 19 April 2006
Available online 3 July 2006

Abstract

Pyrite bearing barite concretions are abundant in black shales of the Early Cambrian Niutitang Formation in China. Barite in these concretions exhibits greatly elevated $\delta^{34}S$ and $\delta^{18}O$ values, averaging $68 \pm 5‰$ and $20 \pm 1‰$, respectively. Such high values indicate precipitation of barite during diagenesis at an advanced stage of bacterial sulphate reduction forming at the ''barite front''. Pyrite sulphur has a relatively constant isotopic composition of $\sim 10‰$ in both concretions and host rock and likely formed prior to barite. Fluctuating methane flux into the zone of anaerobic methane oxidation led to the consumption of sulphate and release of barium into higher sediment layers. During radial concretion growth Ba^{2+} interacted with SO_4^{2-} bearing fluids of various concentrations and isotopic compositions over a prolonged period, resulting in a lack of any systematic correlation between sulphate $\delta^{34}S$ and $\delta^{18}O$ values throughout the concretion.

1. Introduction

Sedimentary barite has often been studied for deciphering past and present, physical and chemical, marine depositional environments. Bréhéret and Delamette (1989) and Bréhéret and Brumsack (2000) demonstrated a definite link between the development of barite concretions and breaks in sedimentation. In marine sediments barite is often used as a paleoproductivity indicator (e.g. Dymond et al., 1992; Paytan et al., 1996; Dean et al., 1997). In addition, sulphur and oxygen stable isotopic ratios and $^{87}Sr/^{86}Sr$ ratios of barite have been used as proxies for past seawater composition (Paytan et al., 1993, 1998; Martin et al., 1995; Strauss, 1997; Turchyn and Schrag, 2004). Sedimentary barite can form by biogenic, diagenetic and hydrothermal pathways (Dean and Schreiber, 1978; Kusakabe et al., 1990; Moore and Stakes, 1990; Torres et al., 1996; Paytan et al., 2002), but only 'biogenic' barite, precipitated directly from seawater in the presence of decaying organic debris (Dehairs et al., 1980; Bishop, 1988; Ganeshram et al., 2003) records the stable isotopic signature of seawater (Paytan et al., 2002). $BaSO_4$ has a very low solubility product of

* Corresponding author. Address: Geologisch-Paläontologisches Institut, Westfälische Wilhelms Universität, Corrensstrasse 24, 48149 Münster, Germany. Tel.: +61 7 4781 4897; fax: +61 7 4725 1501.
E-mail address: tatiana.goldberg@jcu.edu.au (T. Goldberg).

0146-6380/$ - see front matter © 2006 Elsevier Ltd. All rights reserved.
doi:10.1016/j.orggeochem.2006.04.013

1.08×10^{-8} (Rushdi et al., 2000). Most of the water column in the ocean is undersaturated with respect to barite, whereas sulphate depleted pore-waters are commonly oversaturated (Church and Wolgemuth, 1972; Brumsack and Gieskes, 1983; Brumsack, 1986).

Diagenetic barite is thought to form below the sediment–water interface via remobilisation of barium in the zone of sulphate reduction, typically displaying elevated $\delta^{34}S$ and $\delta^{18}O$ values (Dean and Schreiber, 1978; Torres et al., 1996; Lesniak et al., 1999; Raiswell et al., 2002). Recently diagenetic barite has been connected to methane diffusion and its oxidation via sulphate reduction (Arndt et al., 2006). Ba^{2+} has been documented to migrate together with CH_4-rich fluids and precipitate at methane seeps on continental margins (Greinert et al., 2002; Aloisi et al., 2003; Torres et al., 2003), as well as in deeper sedimentary layers (Dickens, 2001; Arndt et al., 2006) resulting in large barite deposits. Upward diffusing CH_4 fluxes and downward diffusing SO_4 result in anaerobic oxidation of methane (AOM) and promote the dissolution of (bio-)barite, due to its low solubility product (Arndt et al., 2006). Together with methane, Ba^{2+} diffuses into the sulphate containing pore water, triggering the precipitation of barite at the sulphate/methane interface (Shipboard Scientific Party, 2002; Torres et al., 2003). In ocean margin sediments AOM is the primary means for CH_4 oxidation and the major sink for SO_4^{2-} (D'Hondt et al., 2002).

In this study we present sulphur and oxygen isotopic compositions of barite and pyrite in barite concretions from the Lower Cambrian Niutitang Formation, Yangtze Platform, China. The results are supported by petrographic studies. Extraordinarily high $\delta^{34}S$ values of 61.6–71.8‰ (mean 67.7‰) of Lower Cambrian barites have already been documented in correlative Jixi barite deposits of the Jiangnan region (Wang et al., 1993). Based entirely on sulphur isotope values, a diagenetic origin was entertained, but not fully explored. Wang and Li (1991) investigated several Lower Cambrian barite deposits across the Yangtze Platform, and postulated a predominantly hydrothermal source for barium; they ascribed high $\delta^{34}S$ values, of up to 50‰, to enrichment via bacterial sulphate reduction. This presumption was based on the comparison of the sulphur isotopic composition to the $\delta^{34}S$–sulphate curve of Holser et al. (1988). Strontium isotope data have been variously interpreted to indicate a hydrothermal origin (Wang and Chu, 1994; Clark et al., 2004) or a diagenetic origin at methane seeps (Torres et al., 2003) for these deposits. Our discussion focuses on the genesis of the Niutitang Formation barite–pyrite concretions in the light of new data and these previous studies.

2. Geological setting and sampling

Barite deposits occur within dark cherts and black shales of the Early Cambrian Niutitang Formation (and stratigraphic equivalents) on the Yangtze Platform in South China. They form laterally across wide parts of the Yangtze Platform and were interpreted to be stratiform deposits (Wang and Li, 1991). The Niutitang Formation comprises mainly black shales, siltstones, intercalated chert, organic-rich carbonates and phosphate nodules (Fig. 2). Deposition of the Niutitang Formation occurred during the Early Cambrian transgressive 'Badaowan–Niutitang' event (Steiner, 2001), leading to widespread deposition of organic rich shales and mudstones across the entire Yangtze Platform (Fig. 1B).

Barite–pyrite concretions and the black mudstone host rocks were sampled from the Niutitang Formation at the Longshancun section near Duoding village, Guizhou province (Fig. 1A). The concretions are well preserved and unweathered, whereas the host rock shows some post-depositional oxidation of pyrite.

Barite nodules are concentrated within the *Tsunyidiscus* Subzone, documented by the occurrence of the trilobites *Tsunyidiscus niutitangensis* and *Tsunyidiscus armatus* (Yang et al., 2003). The Subzone overlies the Small Shelly Assemblage Zone comprising *Sinosachites flabelliformis – Tannuolina zhangwentangi* and the *Parabadiella* Taxon-range Subzone (Steiner, 2001, 2004) belonging to the Qiongzhusian stage, which can be correlated to the Atdabanian Stage of the Lower Cambrian (Zhu et al., 2001). Based on radiometric dating ($^{238}U/^{206}Pb$) and biostratigraphy the Atdabanian–Botomian boundary was set at 525 Ma and the Tommotian–Atdabanian boundary at ~527/528 Ma (Bowring et al., 1993; Grotzinger et al., 1995).

3. Analytical methods

Three well preserved concretions (Duo1, Duo2 and Duo3) were selected for petrographic and chemical analyses. Duo1 and Duo2 were cut into

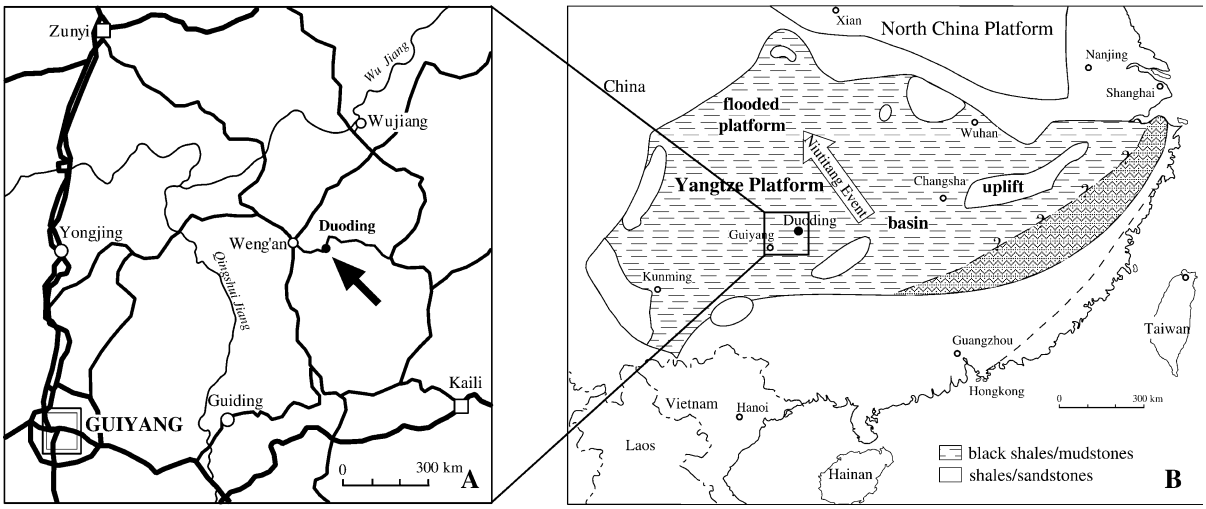

Fig. 1. (A) Geographic setting of the Longshancun section, near Douding, Guizhou Province, China. (B) Paleoenvironmental reconstruction of the Yangtze Platform during Tommotian–early Atdabanian. Modified after Steiner (2001).

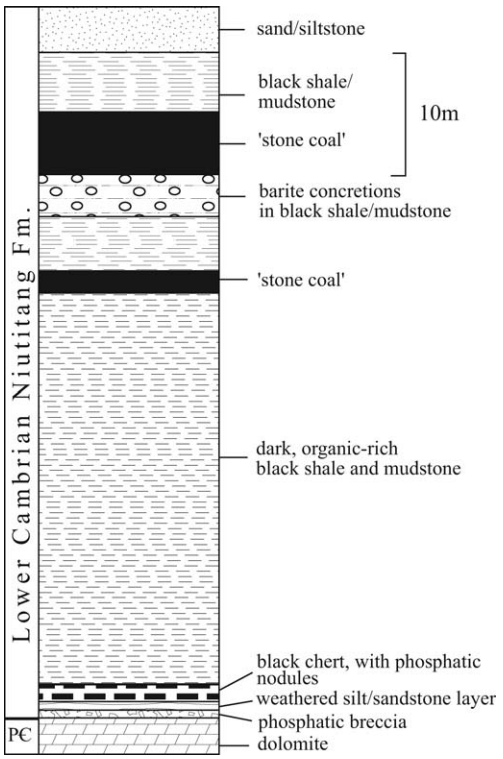

Fig. 2. Lithological profile of the Longshancun section, Niutitang Formation, Guizhou Province.

two halves along the long axis of the concretions. One half was polished for microsampling of pyrite and barite using a dentist's drill with a tungsten carbide bit attachment. Prior to sampling a detailed textural study was performed by using incident and reflected light microscopy. Microsampling was carried out along a traverse from core to rim. Pure barite was separated by stirring for 24 h in a hot 65% HNO_3 solution to dissolve pyrite. Purity of barite was evaluated via X-ray diffractometry (XRD) by comparing the powder spectrum to the standard barite (syn 24-1035*) spectrum. Pyrite was extracted with 1 M chromium chloride solution and 6 N hydrochloric acid in a N_2 atmosphere. Hydrogen sulphide (H_2S) produced by reduction of sulphide was trapped as zinc sulphide in a zinc acetate solution (pH 11) and subsequently reprecipitated as silver sulphide (Ag_2S) by adding $AgNO_3$ (Canfield et al., 1986). Residual powder was treated with Eschka's reagent and combusted at 800 °C. Sulphate was extracted with distilled water and acidified to pH 2. Using an 8.5% $BaCl_2$ solution, barium sulphate ($BaSO_4$) was precipitated. $\delta^{34}S$ of $BaSO_4$ and Ag_2S was measured with a Finnigan Delta-plus mass spectrometer equipped with an elemental analyser (EA) in a continuous flow system. For oxygen isotopic measurements $BaSO_4$ was combusted at 1450 °C in the glassy carbon reactor of a TC/EA-unit connected to the mass spectrometer. Results for S are reported in the standard delta notation against the Canyon Diablo Troilite standard (V-CDT), with reproducibility better than $\pm 0.3‰$. The oxygen isotopic composition was measured against Standard Mean Ocean Water (V-SMOW) and is reproducible to $\pm 0.5‰$. Total organic carbon (TOC) was determined with a CS-MAT 5500 using NDIR spectroscopy as the difference between total and inorganic carbon.

4. Results

4.1. Petrography and mineralogy

The ellipsoidal concretions have a long axis of ca. 13 cm parallel to the bedding plane and a minor axis of ca. 6 cm. Barite and pyrite are the dominant mineral phases, forming as concentric growth rings around the nodule centre (Fig. 3A). Silicates (clays, detrital quartz) are present in trace concentrations. Total organic carbon (TOC) and total inorganic carbon (TIC) contents are ~0.5% and ~0.02%, respectively. The XRD spectrum of the powdered barite concretion margin matched the standard barite spectrum and is therefore close to 100% $BaSO_4$. The crystal size of barite increases from rhombohedral microcrystalline (~50 μm) at the centre to radial-fibrous macrocrystalline (up to 3 mm) towards the rim (Fig. 3B). Only euhedral cubic pyrite could be observed. Pyrite crystals are ~15 μm in size. Visual estimation of mineral content (volume percentages) was made with a petrographic microscope. Polished sections through the concretions reveal concentric layering of pyrite around the core and near the margins (Fig. 3A). Barite content increases from 60% to 95%, whereas pyrite content decreases from 20% to 2% from centre to the margin, respectively. About 10% of an opaque phase could be identified, which is largely organic matter. The host black mudstone contains ~6% TOC and 0.05% pyrite.

4.2. Sulphur and oxygen isotopic compositions

Sulphur isotope data for barite ($\delta^{34}S_{barite}$) and pyrite ($\delta^{34}S_{pyr}$) and oxygen isotopic data for barite ($\delta^{18}O_{barite}$) are listed in Table 1. In Duo-1 $\delta^{34}S_{barite}$ ranges from 63.1‰ to 70.2‰ and $\delta^{18}O_{barite}$ from 20.8‰ to 21.5‰, whereas $\delta^{34}S_{pyr}$ values fall within a narrow range of 8.7–9.9‰. $\delta^{34}S_{barite}$ and $\delta^{18}O_{barite}$ for Duo-2 are slightly higher, ranging from 65.2‰ to 74.5‰ and from 18.7‰ to 20.5‰, respectively. $\delta^{34}S_{Pyr}$ is 8.4–11.9‰. For Duo-3 a sulphur isotope value of 68.3‰ and an oxygen isotope value of 19.3‰ were obtained for the concretion margin. For the host rock $\delta^{34}S_{pyr}$ of 8.5‰ was measured, which is not significantly different from the $\delta^{34}S_{pyr}$ values within the concretions.

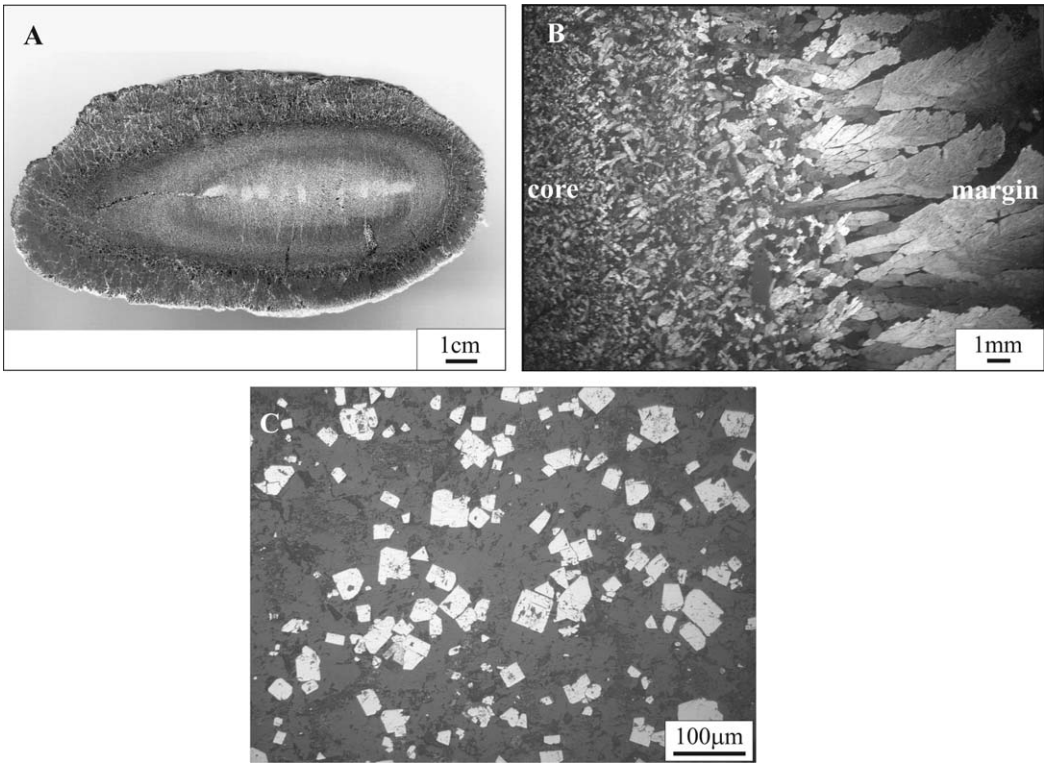

Fig. 3. (A) Barite concretion (Duo-1). (B) Thin section of barite concretion Duo-2 in plane-polarised light, through a polarisation microscope. (C) Thin section of Duo-2, euhedral pyrite crystals in reflected light.

5. Discussion

5.1. Isotopic composition

Sulphate in Niutitang Formation barites in this study is characterised by highly elevated $\delta^{34}S$ and $\delta^{18}O$ values (Fig. 4). Enrichment in ^{34}S in sedimentary concretionary barite has also been reported by Wang et al. (1993), Lesniak et al. (1999), Repcok et al. (2000), Bréhéret and Brumsack (2000) and Raiswell et al. (2002). Repcok et al. (2000) reported $\delta^{34}S_{barite}$ values of up to 105.3‰. The observed sulphur and oxygen isotopic compositions in the present work are considerably higher than those proposed for Early Cambrian seawater $\delta^{34}S$ of 33 ± 3‰ (Claypool et al., 1980; Shields et al., 1999; Kampschulte and Strauss, 2004) and $\delta^{18}O$ of 14 ± 1‰ (Claypool et al., 1980; Goldberg et al., 2005), although the absolute values and range of published evaporite $\delta^{18}O$ data are particularly poorly constrained.

The observed enrichment in sulphur and isotopic compositions can be attributed to bacterial sulphate reduction (BSR) and Rayleigh fractionation (Bottrell and Raiswell, 2000). Bacterially mediated dissimilatory sulphate reduction involves reduction of dissolved SO_4^{2-} to H_2S via a series of complex enzymatically catalyzed biochemical reactions coupled with organic matter oxidation which serves as an electron donor (Berner, 1984; Canfield, 2001). The reductive process within the bacterial cell (APS to sulphite and sulphite to sulphide) causes extensive sulphur isotopic fractionation owing to preferential breakage of ^{32}S–O bonds compared to ^{34}S–O bonds. As a result the H_2S produced during the reaction is enriched in ^{32}S relative to ^{34}S (Harrison and Thode, 1958; Canfield, 2001). Continuous removal of H_2S via precipitation of metal sulphide (commonly pyrite; FeS_2) from the pore water under sulphate limited conditions (closed system) would enrich the residual sulphate in ^{34}S. This enrichment trend can be calculated using a Rayleigh equation of the form $R/R_0 = f^{(\alpha-1)}$, where α is the fractionation factor, and R and R_0 are the $^{34}S/^{32}S$ ratios of residual and initial sulphate in the fluid, respectively.

Experimental studies (Canfield and Thamdrup, 1994; Cypionka et al., 1998; Habicht et al., 1998; Böttcher et al., 2001) involving disproportionation of elemental sulphur (S^0), thiosulphate ($S_2O_3^{2-}$) and sulphite (SO_3^{2-}) demonstrate the possibility of creating a large sulphur isotope fractionation between sulphate and sulphide. Through repeated steps of sulphide oxidation and disproportionation

Table 1

cm from core	$\delta^{34}S$ pyrite (‰)	$\delta^{34}S$ barite (‰)	$\delta^{18}O$ barite (‰)	$\Delta\delta^{34}S/\Delta\delta^{18}O$[a]	$\Delta^{34}S$ (barite–pyrite)
Duo-1					
0.0	8.7	63.1	20.8	4.4	54.4
0.5	9.2	65.9	21.5	4.4	56.8
1.0	10.0	70.2	21.4	5.0	60.3
1.4	9.9	68.1	21.3	4.8	58.2
1.7		66.7	21.5	4.5	
2.3	9.1	68.2	20.8	5.2	59.1
Duo-2					
0.0	8.7	70.5	19.1	7.4	61.7
0.8	10.0	74.5	20.5	6.4	64.5
1.3	10.6	65.2	20.2	5.2	54.6
1.7	11.9	72.2	19.7	6.9	60.4
2.1		67.0	18.8	7.2	
3.0	8.4	66.8	19.3	6.3	58.4

Margin	$\delta^{34}S$ barite (‰)	$\delta^{18}O$ barite (‰)	$\Delta\delta^{34}S/\Delta\delta^{18}O$[a]
Duo-3			
	68.3	19.8	6.1

$\delta^{34}S$ pyrite (‰)	$\delta^{34}S$ OBS (‰)	TOC (wt%)	OBS (wt%)
Host rock			
8.5	44.7	6.0	0.19

[a] Where seawater $S_{SO_4} = 33$‰ and $O_{SO_4} = 14$‰.

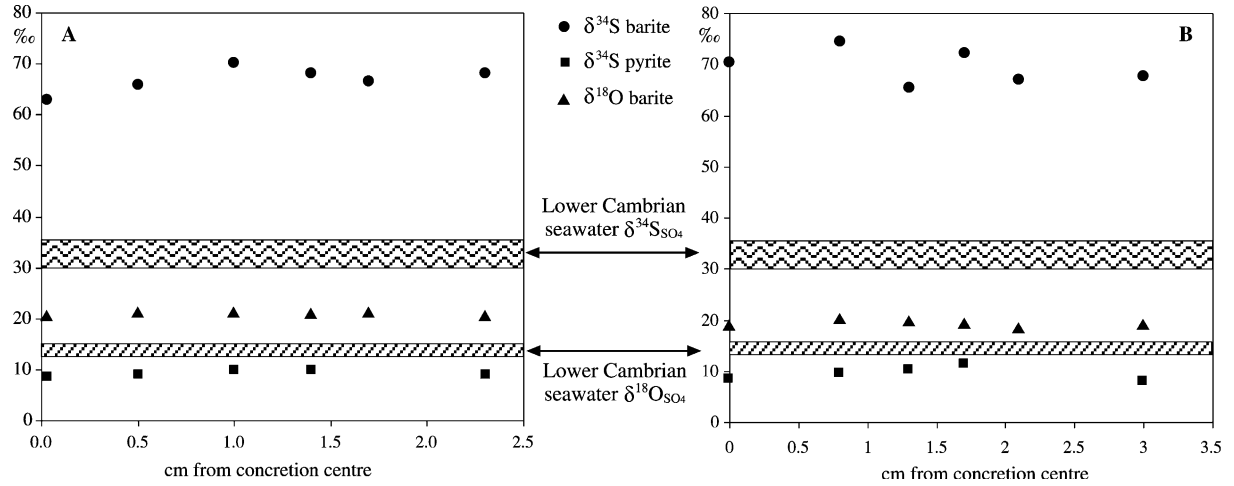

Fig. 4. (A) Plot of $\delta^{34}S$ and $\delta^{18}O$ of barite, and $\delta^{34}S$ of pyrite, from concretion Duo-1 centre to margin. (B) Plot of $\delta^{34}S$ and $\delta^{18}O$ of barite, and $\delta^{34}S$ of pyrite, from concretion Duo-2 centre to margin.

sulphide becomes successively more depleted and the residual sulphate pool more enriched in ^{34}S.

Isotopic enrichment of residual sulphate in ^{34}S is accompanied by corresponding ^{18}O enrichment. A $(\Delta\delta^{34}S/\Delta\delta^{18}O)_{SO_4}$ enrichment ratio of ~4 was proposed to be diagnostic of seawater-derived sulphate whose isotopic composition was modified solely by bacterial sulphate reduction corresponding to the Rayleigh fractionation (Sakai, 1971; Claypool et al., 1980; Mandernack et al., 2003). Alternatively Brunner et al. (2005) refuted a kinetic effect as the dominating mechanism of oxygen isotope fractionation processes and emphasised an equilibrium governed oxygen isotope exchange between cell internal sulphur compounds (APS) and ambient seawater. Furthermore, bacterial disproportionation of intermediate sulphur compounds, results in various $(\Delta\delta^{34}S/\Delta\delta^{18}O)_{SO_4}$ ratios ranging from 0.89 to 1.1 (Aharon and Fu, 2003; Brunner et al., 2005). The second parameter controlling sulphur to oxygen isotopic ratios is the sulphate reduction rate. Low bacterial sulphate reduction rates lead to increased equilibration between sulphate and water, thus decreasing the $(\Delta\delta^{34}S/\Delta\delta^{18}O)_{SO_4}$ ratio and vice versa (Böttcher et al., 1998, 1999; Aharon and Fu, 2000).

In our case, the enrichment ratio is difficult to assess due to a poorly constrained seawater sulphate isotope composition for the Early Cambrian. Taking the above mentioned values of Cambrian seawater $\delta^{34}S$ of 33‰ and $\delta^{18}O$ of 14‰, the calculated enrichment ratio ($(\Delta\delta^{34}S/\Delta\delta^{18}O)_{SO_4}$) would average 5.7, which is improbably high (see above). Such a high value implies that our chosen estimate of Early Cambrian seawater $\delta^{34}S$ is too low and/or that of $\delta^{18}O$ is too high.

Hydrogen sulphide reacts with easily reducible ferric compounds (e.g. iron (oxyhydr)oxide) to form pyrite (FeS_2). Owing to negligible sulphur isotopic fractionation during pyrite precipitation, the pyrite sulphur isotopic composition is representative of its precursor H_2S. Bacterial sulphate reduction under sulphate limited conditions is expected to cause progressive ^{34}S enrichment in pyrite (following Rayleigh equation). Jorgensen et al. (2004) further emphasised that sediment pore-waters always maintain an open system to a certain extent and diffusion of SO_4^{2-} and H_2S plays a major role in the isotopic composition of sulphur. They stated that it is the methane driven sulphate reduction, which is the main source of H_2S formation at depth, that leads to isotopically heavy pyrite in a sediment open to diffusion when combined with a deep H_2S sink. High, but practically constant $\delta^{34}S_{pyr}$ (~+10‰) values recorded in the concretions (from core to margin) suggest, however, a sulphide source with constant or limited range of sulphur isotopic composition. Petrographic observations (see below) also do not support a late diagenetic overgrowth on early diagenetic pyrite. The observed difference between the S isotopic compositions of barite and pyrite ($\Delta^{34}S_{SO_4-pyr}$) of 55–62‰ is larger than can be achieved by bacterial sulphate reduction except in cases of hypersulphidic conditions (Brunner and Bernasconi, 2005; Wortmann et al., 2001) and disproportionation reactions (Canfield, 2001). Because of the lack of correlation

between $\delta^{34}S_{SO_4}$ and $\delta^{34}S_{pyr}$ in our data, and a similar $\delta^{34}S_{pyr}$ between concretional and host rock pyrite a possible explanation for our data (other than disproportionation or hypersulphidic processes) is that the pyrite formed initially during early diagenetic sulphate reduction and was later incorporated into the barite concretion during concretion growth.

5.2. Genesis of barite–pyrite concretions

Interaction of seawater with hydrothermal Ba-enriched fluids, direct precipitation of dissolved Ba and SO_4 in seawater ('bio-barite') and diagenetic formation within the sediments are the principal mechanisms proposed for the genesis of barites (Dean and Schreiber, 1978; Brumsack, 1986; Kusakabe et al., 1990; Moore and Stakes, 1990; Wang and Li, 1991; Torres et al., 1996; Lesniak et al., 1999; Paytan et al., 2002; Raiswell et al., 2002). Barite crystals from this study (~50–3000 μm) are significantly larger than 'biogenic' barite, which forms by precipitation from seawater. Unlike biogenic barite, the barite samples analysed here display higher and more variable $\delta^{34}S$ and $\delta^{18}O$ values than proposed for contemporaneous seawater sulphate.

The possibility of a hydrothermal origin for the barite–pyrite concretions is equally unlikely. Barium derived from hydrothermal Ba-rich fluids reacts immediately with seawater sulphate to precipitate as $BaSO_4$. Such barite crystals are xenomorphic and commonly form rosettes (Paytan et al., 2002). The isotopic composition of hydrothermal barite sulphur is close to the seawater value (Kusakabe et al., 1990; Bréhéret and Brumsack, 2000; Paytan et al., 2002) and oxygen can be ca. 2‰ lower compared to seawater due to sulphate–water equilibrium at high temperatures (Kusakabe et al., 1990). Sulphides, forming from hydrothermal input have $\delta^{34}S$ values around 0–3‰ (Kusakabe et al., 1990). This is inconsistent with our data. Barite crystals from this study show a different morphology and have higher $\delta^{34}S$ and $\delta^{18}O$ than contemporary seawater sulphate. Furthermore, they display higher than hydrothermal pyrite $\delta^{34}S$ values of 8.3–11.9‰.

The barite–pyrite concretions studied here exhibit geochemical and petrographic characteristics suggestive of diagenetic formation within the sediments. High TOC (6 wt%) and organically bound sulphur (0.2 wt%) contents of the host mudstone indicate high preservation potential in an anoxic depositional environment. High abundance of labile organic matter and the presence of sulphate promote rapid sulphate reduction (e.g. Berner, 1984). Resultant H_2S is partitioned into inorganic (pyrite) or organic sulphur phases (OBS) or lost from the sediment by oxidation or diffusion into the upper water column. Modern pyrite weathering may have been responsible for the measured low pyrite abundance in the host sediment. Alternatively (or additionally), low pyrite content (0.02%) and considerably high OBS/pyrite ratio of 8 in the host sediment may indicate iron limitation in the depositional environment. In the absence of easily reducible iron (iron limitation) H_2S is taken up by organic compounds as intra- or intermolecular organosulphur compounds through polysulphide linkages (Werne et al., 2004).

Absence of both framboidal pyrite and secondary overgrowth of pyrite on framboidal precursors within the barite–pyrite concretions suggest single stage pyritisation and slow precipitation rate (Sweeney and Kaplan, 1973; Taylor and Maquacker, 2000) and/or low concentrations of in situ reactive iron (Raiswell, 1982). Pyrite within the nodule centre is present as ~15 μm, euhedral cubic crystals, but crystal size as well as abundance decreases from the centre to the rim of concretions. With progressive crystallisation, iron limitation and/or exhaustion of the dissolved sulphate reservoir in the pore-waters was possibly responsible for very restricted pyritisation at the margin of the barite concretion.

Compared to pyrite, barite crystal size significantly increases from core to margin. This indicates rapid precipitation at the beginning of nodule formation and slow precipitation and limited nucleation sites towards the end of concretion formation. Rapid precipitation was possibly initiated by the availability of sufficient Ba^{2+} and SO_4^{2-} ions exceeding the solubility product of $BaSO_4$, which is extremely low. Concretion growth can proceed concentrically (from the centre towards the rim), or contemporaneously with pervasive sedimentation. Concentric growth of barite nodules has been observed under sulphate limiting conditions and was associated with isotope enrichment in both $\delta^{34}S$ and $\delta^{18}O$ from the centre to the margin of the concretion (Coleman and Raiswell, 1981; Repcok et al., 2000). On the other hand, pervasive growth results in lighter (early diagenetic) pyrite $\delta^{34}S$ in the margin and heavier (late diagenetic) in the concretion centre (Raiswell et al., 2002).

In this study the isotopic proxies do not display a systematic shift across the concretion. Nevertheless,

the most likely growth mechanism of the studied concretions is concentric, as indicated by the described development of barite crystal size and crystal distribution from centre to margin. Furthermore the fairly constant isotopic composition of pyrite $\delta^{34}S$ throughout the nodule implies a separate evolution for pyrite and barite. Initially, small pyrite concretions formed within the black shales decreasing in size radially away from the pyrite concretion, possibly as a result of iron limitation. Barite formed at a later stage, using the pyrite concretion as a nucleus.

The source of barium is difficult to constrain for Lower Cambrian sediments on the Yangtze Platform. However, organic matter degradation and decomposition of phosphatic small shelly fossils and other early organisms may have released barium into sulphate depleted pore-waters. It is also possible that previously deposited biogenic barite from the sedimentary section below was dissolved through the process of sulphate reduction. The dissolved Ba^{2+} diffused upwards in the sediment column and precipitated at the base of the sulphate reduction zone where some residual sulphate still existed, also referred to as the barite front (Brumsack, 1986; Torres et al., 1996; Raiswell et al., 2002). A stable barite front relative to the oxic/anoxic interface for a protracted period of time allows the formation of large concretions. This is generally associated with low sedimentation rates (Dean and Schreiber, 1978; Brumsack, 1986; Bréhéret and Delamette, 1989; Torres et al., 1996; Bréhéret and Brumsack, 2000), where the oxicline is not significantly shifted to higher sediment layers by continuous rapid sedimentation. Torres et al. (1996) further concluded that sedimentation rates should vary and even pause to promote precipitation of large barite deposits or concretions, where barite precipitation occurs at a certain depth interval.

It has also been suggested that high and variable $\delta^{34}S$ in barite reflects different sulphate/sulphide pore-water gradients that result from changing methane fluxes from the underlying black shales over time, and variable anaerobic metabolism of methane by sulphate reducing bacteria (Böttcher et al., 2005). Higher diffusive flux of methane, mirroring a higher rate of methanogenesis, will enhance sulphate reduction via AMO causing the sulphate/methane interface to move upwards and vice versa (Arndt et al., 2006). At the sulphate/methane interface sulphate reduction and methane oxidation are maximal. It has been observed that Ba^{2+} concentration increases at this level owing to dissolution of biobarite (Dickens, 2001; Arndt et al., 2006). Dissolved Ba^{2+} moves up and precipitates as barite crystals (on a nucleus) where the product of sulphate and barium ionic concentrations is greater than the solubility product of $BaSO_4$. If the methane flux is low sulphate will percolate further down and barite will precipitate at a lower level, whereas higher methane flux will move the barite front upwards. This process will also cause some amount of dissolution of the pre-existing barite precipitate. For the growth of large nodules a steady supply of sulphate and barium, throughout prolonged concretion formation time, is required at the nodule growth zone. If the fluctuation is too high it will result in precipitation of dispersed barite crystals over the zone of sulphate reduction. A quasi-steady-state of the sulphate–methane interface is therefore expected. At each point of precipitation, represented by a layer, barite will freeze the isotope composition of in situ pore water residual sulphate and sulphide. Sulphate concentration as well as the isotopic composition of sulphur and oxygen will vary at different barite precipitation stages, as seen in this study. A greater methane flux would enhance the sulphate reduction rate, providing sulphate is sufficient, and lead to increased sulphate reduction. Changes in the methane flux and with it the sulphate reduction rate might have been additionally responsible for the different $(\Delta\delta^{34}S/\Delta\delta^{18}O)_{SO_4}$ ratios (see Section 5).

6. Conclusion

Petrographic and geochemical results for Lower Cambrian barite–pyrite concretions from the Yangtze platform, China indicate a diagenetic origin for these concretions. Pyrite nodules formed at an earlier stage, whereas barite precipitation commenced during the final stages of sulphate reduction at the barite front, indicated by significantly elevated $\delta^{34}S$ and $\delta^{18}O$ values relative to contemporaneous seawater. Concretion growth proceeded concentrically from centre to margin. The lack of correlation and systematic distribution of $\delta^{34}S$ and $\delta^{18}O$ values resulted from variations in the isotopic composition of sulphate in the pore fluid throughout prolonged concretion growth. This isotopic variability is connected to changing methane and sulphate fluxes into the zone of anaerobic methane oxidation.

Acknowledgements

We greatly acknowledge the support by the Deutsche Forschungsgemeinschaft (Str 281/16).

Fieldwork was also supported by the National Science Foundation China and assisted by our Chinese colleagues – Thank You! We appreciate the technical support provided by A. Fugmann during laboratory work. Helpful suggestions by Adina Paytan and Hans Brumsack are cordially acknowledged, as are editorial comments by Michael Böttcher.

References

Aharon, P., Fu, B., 2000. Microbial sulphate reduction rates and sulphur and oxygen isotope fractionations at oil and gas seeps in deepwater Gulf of Mexico. Geochimica et Cosmochimica Acta 64, 233–246.

Aharon, P., Fu, B., 2003. Sulphur and oxygen isotopes of coeval sulphate–sulphide in pore fluids of cold seep sediments with sharp redox gradients. Chemical Geology 195, 201–218.

Aloisi, G., Wallmann, K., Bollwerk, S.M., Derkachev, A., Bohrmann, G., Suess, E., 2003. The effect of dissolved barium on biogeochemical processes at cold seeps. Geochimica et Cosmochimica Acta 68, 1735–1748.

Arndt, S., Brumsack, H.-J., Wirtz, K.W., 2006. Cretaceous black shales as active bioreactors: a biogeochemical model for the deep biosphere encountered during OPD Leg 207 (Demerere Rise). Geochimica et Cosmochimica Acta 70, 408–425.

Berner, R.A., 1984. Sedimentary pyrite formation: an update. Geochimica et Cosmochimica Acta 48, 605–615.

Bishop, J.K.B., 1988. The barite–opal–organic carbon association in oceanic particulate matter. Nature 332, 341–343.

Böttcher, M.E., Brumsack, H.J., de Lange, G.J., 1998. Sulphate reduction and related stable isotope (^{34}S, ^{18}O) variations in interstitial waters from the eastern Mediterranean. In: Robertson, A.H.F., Emeis, K.-C., Richter, C., Camerlenghi, A. (Eds.), Proceedings of the Ocean Drilling Program, Scientific Results, vol. 160, pp. 365–373.

Böttcher, M.E., Bernasconi, S.M., Brumsack, H.J., 1999. Carbon, sulphur, and oxygen isotope geochemistry of interstitial waters from western Mediterranean. In: R. Zahn, Cornas., M.C., Klaus, A. (Eds.), Proceedings of the Ocean Drilling Program, Scientific Results, pp. 413–421.

Böttcher, M.E., Thamdrup, B., Vennemann, T., 2001. Oxygen and sulphur isotope fractionation during anaerobic bacterial disproportionation of elemental sulphur. Geochimica et Cosmochimica Acta 65, 1601–1609.

Böttcher, M.E., Brumsack, H.J., Hetzel, A., Schipper, A., 2005. Sulphur isotope biogeochemistry and iron speciation of sediments from the Demerara rise (ODP Leg 207). Geophysical Research Abstracts 7, 07384.

Bottrell, S.H., Raiswell, R., 2000. Sulphur isotopes and microbial sulphur cycling in sediments. In: Riding, R.E., Awramik, S.M. (Eds.), Microbial Sediments. Springer, Berlin, pp. 96–104.

Bowring, S.A., Grotzinger, J.P., Isachsen, C.E., Knoll, A.H., Pelechaty, S.M., Kolosov, P., 1993. Calibrating rates of early Cambrian evolution. Science 261, 1293–1298.

Bréhéret, J.-G., Brumsack, H.-J., 2000. Barite concretions as evidence of pauses in sedimentation in the Marnes Bleues Formation of the Vocontian Basin (SE France). Sedimentary Geology 130, 205–228.

Bréhéret, J.-G., Delamette, M., 1989. Les nodules barytiques d'âge crétacé moyen dans le domaine vocontien (SE France), marqueurs de discontinuités sédimentaires en série marneuse de bassin. Comptes Rendus de l Academie des Sciences Serie II 308, 1369–1374.

Brumsack, H.-J., 1986. The inorganic geochemistry of Cretaceous black shales (DSDP Leg 41) in comparison to modern upwelling sediments from the Gulf of California. In: Summerhayes, C.P., Shackleton, N.J. (Eds.), North Atlantic Palaeoceanography. Geological Society Special Publications.

Brumsack, H.-J., Gieskes, J.M., 1983. Interstitial water trace metal chemistry of laminated sediments from the Gulf of California, Mexico. Marine Chemistry 14, 89–106.

Brunner, B., Bernasconi, S.M., Kleikemper, J., Schroth, M.H., 2005. A model for oxygen and sulphur isotope fractionation in sulphate during bacterial sulphate reduction processes. Geochimica et Cosmochimica Acta 69, 4773–4785.

Brunner, B., Bernasconi, S.M., 2005. A revised isotope fractionation model for dissimilatory sulphate reduction in sulphate reducing bacteria. Geochimica et Cosmochimica Acta 69, 4759–4771.

Canfield, D.E., 2001. Biogeochemistry of sulphur isotopes. In: Valley, J.W., Cole, D.R. (Eds.), Stable Isotope Geochemistry. Reviews in Minerology and Geochemistry. Geological Society of America, Washington, pp. 607–633.

Canfield, D.E., Thamdrup, B., 1994. The production of ^{34}S-depleted sulphide during bacterial disproportionation of elemental sulphur. Science 266, 1973–1975.

Canfield, D., Raiswell, R., Westrich, J., Reaves, C., Berner, R., 1986. The use of chromium reduction in the analysis of inorganic sulphur in sediments and shales. Chemical Geology 54, 149–155.

Church, T.M., Wolgemuth, K., 1972. Marine barite saturation. Earth and Planetary Science Letters 15, 35–44.

Clark, S.H.B., Poole, F.G., Wang, Z., 2004. Comparison of some sediment-hosted, stratiform barite deposits in China, the United States, and India. Ore Geology Reviews 24, 85–101.

Claypool, G.E., Holster, W.T., Kaplan, I.R., Sakai, H., Zak, I., 1980. Age curves of sulphur and oxygen isotopes in marine sulphate and their mutual interpretation. Chemical Geology 28, 199–206.

Coleman, M.L., Raiswell, R., 1981. Carbon, oxygen and sulphur isotope variations in concretions from the Upper Lias of N.E. England. Geochimica et Cosmochimica Acta 45, 329–340.

Cypionka, H., Smock, A., Böttcher, M.E., 1998. A combined pathway of sulphur compound disproportionation in *Desulfovibrio desulfuricans*. FEMS Microbiological Letters 166, 181–186.

Dean, W.E., Schreiber, B.C., 1978. Authigenic barite, LEG 41, Deep Sea Drilling Project. In: Y. Lancelot, Seibold, E., et al. (Eds.), Initial Reports of Deep Sea Drilling Project, pp. 915–931.

Dean, W.E., Gardner, J.V., Piper, D.Z., 1997. Inorganic geochemical indicators of glacial–interglacial changes in productivity and anoxia of the California continental margin. Geochimica et Cosmochimica Acta 21, 4507–4518.

Dehairs, F., Chesselet, R., Jedwab, J., 1980. Discrete suspended particles of barite and the barium cycle in the open ocean. Earth and Planetary Science Letters 49, 529–550.

Dickens, G.R., 2001. Sulphate profiles and barium fronts in sediment on the Blake Ridge: present and past methane and barium fluxes through a large gas hydrate reservoir. Geochimica et Cosmochimica Acta 65, 529–543.

D'Hondt, S., Rutherford, S., Spivack, A.J., 2002. Metabolic activity of subsurface life in deep-sea sediments. Science 295, 2067–2070.

Dymond, J., Suess, E., Lyle, M., 1992. Barium in deep sea sediments: a geochemical proxy for paleoproductivity. Paleoceanography 7, 163–181.

Ganeshram, R.S., Francois, R., Commeau, J., Brown-Leger, S.L., 2003. An experimental investigation of barite formation in seawater. Geochimica et Cosmochimica Acta 67, 2599–2605.

Goldberg, T., Poulton, S.W., Strauss, H., 2005. Sulphur and oxygen isotope signatures of late Neoproretozoic and early Cambrian sulphate, Yangtze Platform, China: diagenetic constraints and seawater evolution. Precambrian Research 137, 223–241.

Greinert, J., Bollwerk, S.M., Derkachev, A., Bohrmann, G., Suess, E., 2002. Massive barite deposits and carbonate mineralization in the Derugin Basin, Sea of Okhotsk: precipitation processes at cold seep sites. Earth and Planetary Science Letters 203, 165–180.

Grotzinger, J.P., Bowring, S.A., Sylor, B.Z., Kaufman, A.J., 1995. Biostratigraphic constraints on early animal evolution. Science 270, 589–604.

Habicht, K.S., Canfield, D.E., Rethmeyer, J., 1998. Sulphur isotope fractionation during bacterial sulphate reduction and disproportionation of thiosulphate and sulphite. Geochimica et Cosmochimica Acta 62, 2585–2595.

Harrison, A.G., Thode, H.G., 1958. Mechanism of the bacterial reduction of sulphate from isotopic fractionation studies. Transactions of the Faraday Society 54, 84–92.

Holser, W.T., Schidlowski, M., Mackenzie, F.T., Mynard, J.B., 1988. Geochemical cycles of carbon and sulphur. In: Gregor, C.B., Garrels, R.M., Mackenzie, F.T., Maynard, J.B. (Eds.), Chemical Cycles in the Evolution of the Earth. Wiley, New York, pp. 105–173.

Jorgensen, B.B., Böttcher, M.E., Lüshen, H., Neretin, L.N., Volkov, I.I., 2004. Anaerobic methane oxidation and a deep H_2S sink generate heavy sulphides in Black Sea sediments. Geochimica et Cosmochimica Acta 68, 2095–2118.

Kampschulte, A., Strauss, H., 2004. The sulphur isotopic evolution of Phanerozoic seawater based on the analysis of structurally substituted sulphate in carbonates. Chemical Geology 204, 255–286.

Kusakabe, M., Mayeda, S., Nakamura, E., 1990. S, O and Sr isotope systematics of active vent materials from the Mariana backarc basin spreading axis at 18°N. Earth and Planetary Science Letters 100, 275–282.

Lesniak, P.M., Lacka, B., Krajewski, K.P., Hladikova, J., Zielinski, G., 1999. Origin of barite concretions in the West Carpathian flysch, Poland. Chemical Geology 158, 155–163.

Mandernack, K.W., Krouse, H.R., Sklei, J.M., 2003. A stable sulphur and oxygen isotopic investigation of sulphur cycling in an anoxic marine basin, Framvaren Fjord, Norway. Chemical Geology 195, 181–200.

Martin, E.E., Macdougall, J.D., Herbert, T.D., Paytan, A., Kastner, M., 1995. Strontium and neodymium isotopic analysis of marine barite separates. Geochimica et Cosmochimica Acta 7, 1353–1361.

Moore, W.S., Stakes, D., 1990. Ages of barite–sulphide chimneys from the Mariana Trough. Earth and Planetary Science Letters 100, 265–274.

Paytan, A., Kastner, M., Martin, E.E., Macdougall, J.D., Herbert, T., 1993. Marine barite as a monitor of seawater strontium isotope composition. Nature 336, 445–449.

Paytan, A., Kastner, M., Chavez, F.P., 1996. Glacial to interglacial fluctuations of productivity in the equatorial Pacific as indicated by marine barite. Science 274, 1355–1357.

Paytan, A., Kastner, M., Campbell, D., Thiemens, M.H., 1998. Sulphur isotopic composition of Cenozoic seawater sulphate. Science 282, 1459–1462.

Paytan, A., Mearon, S., Cobb, K., Kastner, M., 2002. Origin of marine barite deposits: Sr and S isotope characterisation. Geology 30, 747–750.

Raiswell, R., 1982. Pyrite texture, isotope composition, and the availability of iron. American Journal of Science 275, 636–652.

Raiswell, R., Bottrell, S.H., Dean, S.P., Marschall, J.D., Carr, A., Hatfield, D., 2002. Isotopic constraints on growth conditions of multiphase calcite–pyrite–barite concretions in Carboniferous mudstones. Sedimentology 49, 237–254.

Repcok, I., Misik, M., Elias, K., Ferencikova, E., Harcova, E., Jablonsky, J., Rucka, I., 2000. Extremely isotopically heavy sulphur in barite concretions from Slovakia. Geologica Carpathica Bratislava 51, 301–308.

Rushdi, A., MacManus, J., Collier, R., 2000. Marine barite and celestite saturation in seawater. Marine Chemistry 69, 19–31.

Sakai, H., 1971. Sulphur and oxygen isotopic study of barite concretions from banks in the Japan Sea of Northeast Honshu, Japan. Geochemical Journal 5, 79–93.

Shields, G., Strauss, H., Howe, S., Siegmund, H., 1999. Sulphur isotope composition of sedimentary phosphorites from the basal Cambrian of China: implications for Neoproterozoic–Cambrian biochemical cycling. Journal of Geological Society 156, 943–955.

Shipboard Scientific Party, 2002. Leg 201 Preliminary Report. Controls on Microbial Communities in Deeply Buried Sediments, Eastern Equatorial Pacific and Peru Margin Proceedings of the Ocean Drilling Program, Initial Reports 207, pp. 1–84.

Steiner, M., 2001. The facies development and fossil distribution of the Yangtze Platform (South China) in the Neoproterozoic/earliest Cambrian. Freiberger Forschungshefte C 492, 1–26.

Steiner, M., 2004. Neoproterozoic to early Cambrian small Shelly Faunas of the Yangtze Platform (China) and their biostratigraphic potential for regional and international correlation. In: Zhu, M., Strauss, H., Erdtmann, B.-D. (Eds.), Environmental and Biological Processes of the Cambrian Explosion, Nanjing, pp. 56–57.

Strauss, H., 1997. The isotopic composition of sedimentary sulphur through time. Palaeogeography, Palaeoclimatology, Palaeoecology 132, 97–118.

Sweeney, A.M., Kaplan, I.R., 1973. Pyrite framboid formation: laboratory synthesis and marine sediments. Economic Geology 68, 618–634.

Taylor, K.G., Maquacker, J.H.S., 2000. Early diagenetic pyrite morphology in a mudstone dominated succession: the Lower Jurassic Cleveland Ironstone Formation, eastern England. Sedimentary Geology 131, 77–86.

Torres, M.E., Brumsack, H.J., Bohrmann, G., Emeis, K.C., 1996. Barite fronts in continental margin sediments: a new look at

barium remobilisation in the zone of sulphate reduction and formation of heavy barites in diagenetic fronts. Chemical Geology 127, 125–139.

Torres, M.E., Bohrmann, G., Dubé, T.E., Poole, F.G., 2003. Formation of modern and Paleozoic stratiform barite at cold methane seeps on continental margins. Geology 31, 897–900.

Turchyn, A.V., Schrag, D., 2004. Oxygen isotope constraints on the sulphur cycle over the past 10 million years. Science 303, 2004–2007.

Wang, Z., Li, G., 1991. Barite and witherite deposits in Lower Cambrian shales of South China: Stratigraphic distribution and geochemical characterisation. Economic Geology 86, 354–363.

Wang, Z., Chu, X., 1994. Strontium isotopic composition of the early Cambrian barite and witherite deposits. Chinese Science Bulletin 39, 52–55.

Wang, Z., Chu, X., Li, Z., 1993. Geological explanation on extraordinary high $\delta^{34}S$ values in a bedded barite deposit of Jixi County, Anhui Province. Scientia Geologica Sinica 2, 249–251.

Werne, J.P., Hollander, D.J., Lyons, T.W., Sinninghe Damsté, J.S., 2004. Organic sulphur biogeochemistry: recent advances and future research directions. In: Amend, J.P., Edwards, K.J., Lyons, T.W. (Eds.), Sulphur Biogeochemistry-Past and Present. Geological Society of America, Boulder, pp. 135–150, Special Paper 379.

Wortmann, U.G., Bernasconi, S.M., Böttcher, M.E., 2001. Hypersulphidic deep biosphere indicates extreme sulphur isotope fractionation during single-step microbial sulphate reduction. Geology 29, 647–650.

Yang, A., Maoyan, Z., Zhang, J., Li, G., 2003. Early Cambrian eodiscoid trilobites of the Yangtze Platform and their stratigraphic implications. Progress in Natural Science 13, 861–866.

Zhu, M., Li, G., Zhang, J., Steiner, M., Qian, Y., Jiang, Z., 2001. Early Cambrian stratigraphy of east Yunnan, south-western China: a synthesis. Acta Palaeontologica Sinica 40 (Suppl.), 4–39.